Tutor

Dr. Jordi Cirera Fernández
Departament de Química Inorgànica i Orgànica

Grau de Química

Treball Final de Grau

Stereochemical influence on tuning the transition temperature in Spin-Crossover molecules.

Efecte de l'estereoquímica en la modulació de la temperatura de transició en molècules amb transició de spin.

Carlota Alcocer Bernuz

January 2024

UNIVERSITAT DE BARCELONA

B:KC Barcelona Knowledge Campus
Campus d'Excel·lència Internacional

Pick a flower on earth and you move the farthest star.

Paul Dirac

I would like to express my sincere appreciation:

To Dr. Cirera, for his help and motivation during the project. Thanks for helping me overcome my fear of computational chemistry and making me fall in love with this world.

To my mother, for being my mainstay all these years and supporting me in everything I set my mind to.

To Javi, because he is always there for me despite our frequent fights.

To Carles, for the patience and love during these last months.

And finally, I would like to mention my father, my farthest star, I am sure he would have been fascinated by this project.

REPORT

CONTENTS

1. SUMMARY

Spin-crossover molecules have been a subject of interest for chemists and physicists ever since they were first reported. The intrinsic technological applications of these systems have made them the focus of intense research. The change in the spin state of the metal center, which can be induced by different stimuli, comes with a notable change in the physical properties of the molecule, such as changes in the magnetic moment, the absorption spectra, and the coordination geometry, thus making these systems ideal candidates for molecular level-based switches.

A key parameter in the characterization of such systems is the transition temperature, $T_{1/2}$, which is the temperature with an equal population of both spin states. It has been shown experimentally that different isomers of Iron (II) systems with bidentate ligands exhibit differences in their spin-crossover properties, also affecting the $T_{1/2}$. This fact reveals the possibility of having an interplay between geometry and magnetic properties.

This work focuses on the modeling of [Fe(1-methyl-2-(pyrimidin-2-yl)-1*H*-benzo[*d*]imidazole)$_3$]$^{2+}$ and [Fe(phenanthroline)$_2$(NCS)$_2$] complexes, studying the differences the *fac* vs. *mer*, and *cis* vs. *trans* isomers show on the transition temperature and other thermochemical parameters associated with the spin transition, aiming to compare the results with the experimental data.

Keywords: Spin-Crossover, Transition Temperature, Density Functional Theory, Stereochemistry, Electronic Structure.

2. RESUM

Les molècules amb transició d'espín han estat un tema d'interès per a químics i físics des que aquest tipus de sistemes van ser descrits per primer cop. Les aplicacions tecnològiques intrínseques d'aquests sistemes els han convertit en el focus d'una recerca intensa. El canvi en l'estat d'espín del centre metàl·lic, que pot ser induït per diferents estímuls, implica un canvi notable en les propietats físiques de la molècula, com els canvis en el moment magnètic, els espectres d'absorció i la geometria de coordinació, fent que aquests sistemes siguin candidats ideals per a commutadors basats en el nivell molecular.

Un paràmetre clau en la caracterització d'aquests sistemes és la temperatura de transició, $T_{1/2}$, aquesta és la temperatura amb la mateixa població d'ambdós estats d'espín. S'ha demostrat experimentalment que diferents isòmers de sistemes de ferro (II) amb lligands bidentats presenten diferències en les seves propietats de transició d'espín, que també afecten la $T_{1/2}$. Aquest fet revela la possibilitat que existeixi interacció entre la geometria i les propietats magnètiques.

Aquest treball s'enfoca en la modelització de complexos [Fe(1-metil-2-(pirimidin-2-il)-1*H*-benzo[*d*]imidazole)$_3$]$^{2+}$ i [Fe(fenantrolina)$_2$(NCS)$_2$], estudiant les diferències que mostren els isòmers *fac* vs. *mer*, i *cis* vs. *trans* en la temperatura de transició i altres paràmetres termoquímics associats a la transició de spin, amb l'objectiu de comparar els resultats amb les dades experimentals.

Paraules clau: transició de spin, temperatura de transició, teoria del funcional de la densitat, estereoquímica, estructura electrònica.

3. IDENTIFICATION AND REFLECTION ON THE SUSTAINABLE DEVELOPMENT GOALS (SDGS)

This project plays an active role in the university's commitment to the Sustainable Development Goals (SDGs) adopted by all United Nations Member States within the 2030 Agenda.[1]

As previously stated, this field has a broad range of applications, most of which are in the technology sector. This project promotes the development of new technologies, research, and innovation towards the goal of prosperity, thereby supporting the 9th objective: Industry, Innovation, and Infrastructure.

This work also contributes to the 12th objective, which stands for Responsible Consumption and Production. The project is founded on computational studies and employs only computer-based tools, leading to minimizing waste production and decreasing environmental impact to near zero.

Figure 1. SDGs pictograms.

4. INTRODUCTION

4.1. SPIN-CROSSOVER PHENOMENON

Spin-crossover (SCO) phenomenon takes place in $3d^4$-$3d^7$ transition metal complexes, involving the switching process between two molecular spin states, the so-called high-spin (HS) and low-spin (LS) configurations (Figure 2). There are practically no SCO examples known with 4*d* and 5*d* transition elements. The octahedral 4*d* and 5*d* complexes show a strong tendency to adopt LS configuration. Tetrahedral SCO complexes of 3*d* elements are not known because the ligand strength is only about half that of octahedral complexes, thus favoring HS behavior.

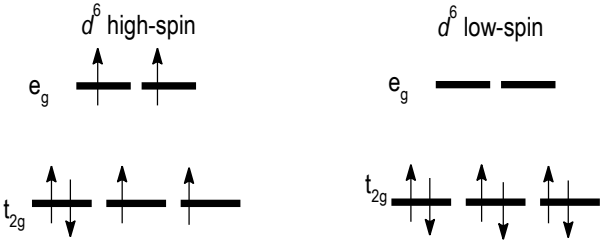

Figure 2. Molecular orbitals d^6 representation for octahedral coordination geometry in both HS and LS.

In the presence of a ligand field, the *d* orbitals undergo a splitting in energy due to the interaction with the ligands. There are two mentioned spin states, depending on the strength of the ligand field. For weak ligand field situations, the energy splitting is smaller than the electron pairing energy, consequently originating a high-spin (HS) state complex with maximum spin multiplicity. Otherwise, in strong ligand field situations, the energy splitting is larger than the electron pairing energy, leading to the low-spin (LS) state complex. There are some cases where the energy splitting is nearly equal to the electron-pairing energy (Figure 3).

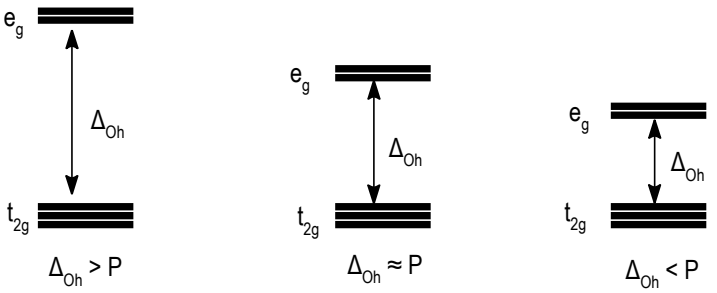

Figure 3. Molecular orbitals scheme for octahedral coordination geometry.
Δ_{Oh}: energy splitting; P: mean electron-pairing energy

SCO phenomenon occurs when the energy difference between the high-spin state and the low-spin state for a given metal is ~k_BT (where T is the temperature and k_B is the Boltzmann constant). When this criterion is fulfilled, switching between spin states on a molecular level can be stimulated using changes in temperature or pressure, and in some cases by irradiation with light. Thermally-induced SCO is also known as spin transition (ST).[2]

4.1.1. SCO thermodynamic definition

In those cases where the energy splitting is similar to the electron-pairing energy, there are two electronic states very close in energy, and it is possible to switch from one spin state to the other by applying an external perturbation. This transition is controlled by a change in the free energy, described as:

$$\Delta G = G^{HS} - G^{LS} = \Delta H - T\Delta S \quad (1)$$

The enthalpic term can be described here as the energy difference between the two electronic spin states. The entropic term should always be positive because of the increasing population of antibonding orbitals going from LS to HS configuration. Therefore, at a specific temperature $\Delta H = T\Delta S$, meaning there is an equilibrium between HS and LS states, both are populated in the same proportion, corresponding to $\Delta G = 0$. This equilibrium temperature, known as the spin transition temperature ($T_{1/2}$), can be determined from:

$$T_{1/2} = \Delta H/\Delta S \quad (2)$$

When it comes to computing the $T_{1/2}$, the free energy expression must be rewritten considering both the electronic and vibrational contributions.

$$\Delta G = \Delta E_{el} + \Delta E_{vib} - T\Delta S \quad (3)$$

Where the electronic contribution is calculated by subtracting electronic energy of LS from electronic energy of HS: $\Delta E_{el} = E_{el}^{HS} - E_{el}^{LS}$.[3]

4.1.2. Physical characterization of SCO complexes

Spin transition in SCO coordination compounds leads to changes in the molecular properties, such as magnetic, optical, vibrational, structural, and thermodynamic changes, being the last the most important ones. Since the earliest spin-crossover (SCO) complexes were presented, every characterization technique has been exploited to understand the nature of these materials.[2]

4.1.2.1. Magnetic susceptibility

Measuring the magnetic susceptibility as a function of temperature, χ_M(T), has been a standard method from the beginning of SCO research, because the change in the number of unpaired electrons between the HS and LS states is reflected in a drastic change of χ_M. It is common to represent the μ_{eff} ($\mu_{eff} = \sqrt{n(n+2)}$, where n is the number of unpaired electrons) curve as a function of the temperature to characterize the magnetic change associated with the change in the spin state. Iron (II) complexes give μ_{eff} values around 0 for the LS and values around 5.0-6.0 for the HS.[2] Transitions in the solid phase are usually abrupt, while in solution the transition is more gradual.[4-5]

4.1.3. SCO behavior of Iron (II) complexes

Mononuclear Iron (II) octahedral SCO complexes are indeed the most widely studied examples of SCO behavior. The electronic configuration of Iron (II) compounds is d^6, meaning that magnetic properties change depending on the spin state. On the one hand, in the LS state, the electronic configuration is $(t_{2g})^6(e_g)^0$, which corresponds to a diamagnetic. On the other hand, in the HS state, the electronic configuration is $(t_{2g})^4(e_g)^2$, corresponding to a paramagnetic.

Intramolecular and intermolecular interactions such as hydrogen bonding and π-π interactions can affect the SCO which leads to difficulty in designing cooperative SCO systems. As a result, the same iron (II) spiral architecture can have a different SCO behavior depending on solvent or counter anions.[6]

4.1.4. SCO applications

Spin-crossover active transition metal complexes are an important class of switchable molecular materials due to their bistable spin-state switching characteristics at or around room temperature.

Since the change in spin state leads to changes in magnetic, optical, and structural properties, there has been considerable interest in the potential of SCO complexes as molecular switches, magnetic storage devices, laser displays, and, more recently, intelligent contrast agents for Magnetic Resonance Imaging .[7]

Despite much progress made and device architectures fabricated, the chemical synthesis of designer functional sublimable SCO complexes is still in its infancy. In this regard, it is desirable to design SCO complexes with additional physical properties thus more systematic efforts are warranted in this direction.[8]

4.2. DENSITY FUNCTIONAL THEORY

When it comes to describing the electronic structure of many-body systems, density functional theory (DFT) is usually the preferred computational method out of all the available methods. Unlike wave function methods, such as Hartree-Fock (HF), DFT provides highly accurate results for calculations in which the energy surface is the quantity of primary interest. It attempts to address both the inaccuracy of Hartree-Fock and the high computational demands of post-Hartree-Fock methods by replacing the many-body electronic wavefunction with the electronic density as the basic quantity.

Modern DFT rests on two theorems by Hohenberg and Kohn (1964). The first theorem states that the ground-state electron density uniquely determines the electronic wavefunction, hence all ground-state properties of an electronic system. The second theorem establishes that the energy of an electron distribution can be described as a function of the electron density, and this function is a minimum for the ground-state density. DFT's main drawback is the unavailability of precise functionals for exchange and correlation, except for the free electron

gas. Nevertheless, many approximations allow the calculation of molecular properties with various levels of precision.[9]

4.2.1. Exchange-correlation functionals

The major problem of DFT is that, except for the free electron gas, exact functionals for exchange and correlation are not known. However, many approximations exist, which allow the calculation of molecular properties at various levels of accuracy. As the exchange-correlation functional is approximated in separate ways, it is necessary to perform a benchmark to choose the most appropriate method for each specific problem.

4.2.1.1. Local density approximation

The most fundamental and simplest approximation is the local-density approximation (LDA), in which the energy depends only on the density at the point where the functional is evaluated, which proved to be an improvement over HF.[9]

The LDA has proven to be a remarkably fruitful approximation. Properties such as structure, vibrational frequencies, elastic moduli, and phase stability (of similar structures) are described reliably for many systems. However, in computing energy differences between different structures, the LDA can have significant errors.[10]

4.2.1.2. Generalized gradient approximation

Functionals belonging to the so-called generalized gradient approximation (GGA) incorporate a dependence not only on the electron density but also on its gradient, thus being able to better describe the inhomogeneous nature of molecular densities. In the GGA, a functional form is adopted, which ensures the normalization condition and that the exchange hole is negative definite. It leads to an energy functional that depends on the density and its gradient but retains the analytic properties of the exchange-correlation hole inherent in the LDA.

4.2.1.3. Meta-GGA and hybrid functionals

The next major step in the development of DFT was the introduction of hybrid functionals, which mix GGA with exact HF exchange. More recent theoretical and methodological developments incorporate the meta-GGA functionals, which extend the GGA corrections to higher derivatives, and the double hybrid functionals, which contain not only a fraction of exact exchange but also a fraction of orbital-dependent nonlocal correlation energy estimated at the level of second-order many-body perturbation theory. An example of a hybrid functional would

be the TPSSh (Tao-Perdew-Staroverov-Scuseria hybrid), which is a meta-GGA functional with a 10% HF mixture.

5. OBJECTIVES

This essay aims to study the influence stereochemistry has on the thermochemical parameters and the transition temperature of spin-crossover molecules. Specifically, study complexes with Iron (II) as a metallic center and with bidentate ligands, the difference between *fac* vs. *mer*, and *cis* and trans isomers. The origin of such differences will be traced back to the underlying electronic structure of the systems, pinpointing its origin and extracting the relationship that optical control can have over the magnetic properties of such systems.

The purpose of the work is to construct the valence orbitals of each molecule to analyze how they are affected by stereochemistry. Comprehending the theoretical background of the project and learning how to operate using DFT methods are among the student's objectives.

6. METHODOLOGY

To begin, the first step is to choose the structures of study. As the goal is to approach the properties differences given by stereochemistry, four molecules taken from the literature[11-12] are the objective of the study. All molecules have Iron (II) as a metallic center and present SCO behavior.

The main problem comes with getting spin state energy gaps as accurate as possible, meaning that calibration must be done before the analysis to see what works and what does not work on the selected molecules of study.

6.1. COMPUTATIONAL MODELLING OF THE STUDIED SYSTEMS

The molecules are constructed using the Gauss View program. It also provides the coordinates of every atom of the molecule. These coordinates are necessary to create the input files of further DFT calculations.

6.2. STRUCTURE MINIMIZATION AND THERMOCHEMISTRY

With the aim of reducing the energy difference between spin states to $\Delta E = k_B T$ (Figure 4), that means getting the ground-state or minimum energy of the molecule, the next step is to optimize its geometry. This is carried out with the Gaussian 09 optimization calculation. The file created must contain the geometry of the molecule extracted from the Gauss View program previously mentioned.

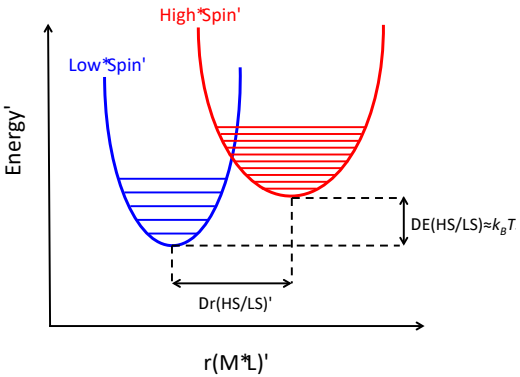

Figure 4. Relative positions of both LS (blue) and HS (red).

In this file, the basis set and the functional is also selected, meaning that it is necessary to prepare these files before all the benchmark parts. Once the molecule is fully optimized, the system offers an output file from which to get the ground-state energy.

After the optimization, a frequency input file is constructed. This file is almost equal to the optimization file, so the easiest way to work is by modifying this file. Furthermore, the frequency cannot be calculated until the optimization has not finished, because it starts from the fully optimized geometry. With the frequency input file, a vibrational calculation is done, it provides thermochemical data, the energy corrected, the enthalpy, and the entropy of the system.

Knowing these values, the transition temperature can be easily calculated using expression 2 from section 4.1.1.

6.3. FUNCTIONAL SCREENING

As a first step of the benchmark, we need to select an exchange correlation functional that reproduces the experimental data. Literature benchmark suggests that TPSSh, OLYP, OBPE and B3LYP* are all suited functionals for spin-state energy gaps. Therefore, the performance of the existing functionals is evaluated using one of the complexes.

As a benchmark system, we used the *fac*-$[Fe(L_1)_3]^{2+}$ (being L_1: 1-methyl-2-(pyrimidin-2-yl)-1*H*-benzo[*d*]imidazole) system, which in solution has an experimental value[11] for $T_{1/2}$ = 309K. Thus, we fully optimized the system of study using all the above functionals in both spin-states (S = 0 and S = 2) in vacuum, performed thermochemical analysis, and computed the transition temperatures. All the data is summarized in Table 1.

Functional	ΔE [kcal/mol]	ΔH [kcal/mol]	ΔS [cal/K·mol]	$T_{1/2}$ [K] calculated	$T_{1/2}$ [K] experimental	Error [K]
TPSSh	7.69	8.94	19.436	460	309	151
OLYP	-1.23	0.14	24.150	6	309	303
OPBE	2.47	3.90	20.835	188	309	121
B3LYP*	1.41	2.67	21.220	126	309	183

Table 1. Calculated thermodynamic parameters using different functionals.

As can be seen, all functionals correctly reproduce the position of the spin-states, the low-spin below the high-spin, reporting a positive value for ΔH. However, the OLYP functional provides a very small value, thus underestimating the SCO behavior. The remaining functionals do a better job and provide $T_{1/2}$ within the range of the experimental value. TPSSh overestimates the experimental value by 151K. From that point of view, in principle any of these options (TPSSh, OPBE and B3LYP*) will be suited for our calculations.

6.4. BASIS SET CALIBRATION

We also explored the convergence of the calculations with the size of the basis set. The choice of the basis set for quantum chemical calculations is remarkably important. To find the best basis set there are two key factors that make us determine which one is the most

appropriate to choose. The first one is the accuracy of the results the basis provides. The other factor we take into consideration is the cost of the calculation. The bigger the basis set is, the more accurate results it offers, but also the higher computational costs it has, meaning it takes more resources and more time to complete the calculation.

It is sometimes possible to use small basis sets to obtain good chemical accuracy, but calculations can often be significantly improved by the addition of diffuse and polarization functions.

In this case the molecule used was the *mer*-$[Fe(L_2)_3]^{2+}$ (being L_2: 1-methyl-2-(pyrimidin-4-yl)-1*H*-benzo[*d*]imidazole), also extracted from the literature. Table 2 displays the obtained results for each of the bases selected.

Basis set	**Basis**	**Number of bases**	**ΔE** [kcal/mol]	**ΔH** [kcal/mol]	**ΔS** [cal/K·mol]	**$T_{1/2}$ [K] calculated**
1	Def2TZV	792	12.03	10.67	16.362	652
2	Def2SVP	853	7.58	6.63	17.561	377
3	Def2QZV	1086	11.68	10.63	15.892	669
4	Def2TZVP	1713	9.16	8.11	17.160	473
5	Def2QZVP	3720	8.21	-	-	-

Calculation of Basis Set Number 5 frequency did not finish due to the extremely high computational cost of the process.

(a) TZV: All-electron valence triple zeta functions
(b) SVP: Split-valence plus polarization functions
(c) QZV: All-electron valence quadruple zeta functions
(d) TZVP: All-electron valence triple zeta plus polarization functions
(e) QZVP: All-electron valence quadruple zeta plus polarization functions

Table 2. Energy difference between HS and LS states and thermochemical analysis for each basis set

Comparing the values obtained for $T_{1/2}$ with the experimental transition temperature value[11] of the system, which is around 341K. Leaving aside basis set number 2, the basis set that came closer to the experimental value was the number 4. Moreover, if we focus on the energy difference between LS and HS, the lowest value is the value obtained using basis set 5, but this basis was disregarded because it took too much time. Def2SVP basis is also dismissed because it works differently and by construction cannot be compared with the rest of the basis for making the extrapolation to the basis set limit. After this evaluation, the final basis set chosen was number 4. It is interesting to mention that the solvent interaction is not taken into consideration in this part of the benchmark.

6.5. PROGRAM DEVELOPMENT

With the backing of Dr. Cirera, a Python program able to calculate free energy, $T_{1/2}$, and the magnetic moment of the system with the data taken from the outputs was developed. Before executing the program, which is explained below, it is necessary to create a text file containing all the frequencies of the HS state, another text file for the frequencies of the LS state, and finally, a text file with the thermochemistry data (zero-point energies, thermal energies, thermal enthalpies, and thermal free energies).

The program starts reading the frequencies and energies of both spin states from the text files created. Then, it requests the user a temperature range (lowest and highest temperature on the interval) and the number of points desired on the interval. After that, the free energy is calculated as a function of the temperature for LS and HS separately, using the expression:

$$G^S(T, v_i^S) = E + k_B T \sum_i \ln\left(1 - e^{-(hv_i/k_B T)}\right) \quad (4)$$

Finally, total free energy is calculated by: $\Delta G(T) = G^{HS}(T, v_i^{HS}) - G^{LS}(T, v_i^{LS})$. Once free energy is calculated it is possible to calculate $T_{1/2}$ and the magnetic moment (μ_{eff}) of the spin state. At the end of the program, the curve of magnetic moment depending on temperature is represented (Figure 5).

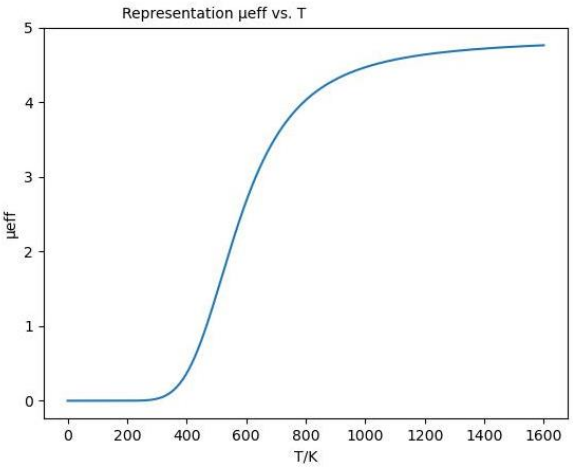

Figure 5. Python μeff vs. Temperature curve representation of the *fac*-$[Fe(L_1)_3]^{2+}$ with CH_3CN as solvent.

For further information, the full program is available in Appendix 1.

6.6. MOLECULAR ORBITALS

The construction of molecular orbitals (MO) diagrams can be highly useful in the discussion of the spin state tendency of the molecules. They give a visual idea of the energy difference between non-bonding t_{2g} orbitals and antibonding e_g orbitals.

On this occasion, the MO diagrams are constructed from the LS state. The frequency checkpoint file is opened with the IQmol program. This program can draw the electronic density of the orbitals from the molecule selected by the user and indicates the HOMO and LUMO. With this help is quite simple to select the coordinate axis and see the number of the desired *d* orbitals, corresponding to the metal d_{xy}, d_{xz}, d_{yx}, d_{z^2}, and $d_{x^2-y^2}$ orbitals. Once known the orbital numbers the first energy of each one is extracted from the output file. All the data is treated with Excel and the representation of the orbitals is also performed with Excel.

7. RESULTS AND DISCUSSION

The optimization of the complexes can be performed once the system is calibrated, and the calculation method is properly chosen. The four molecules selected can be grouped in pairs since they are isomers (Figure 6).

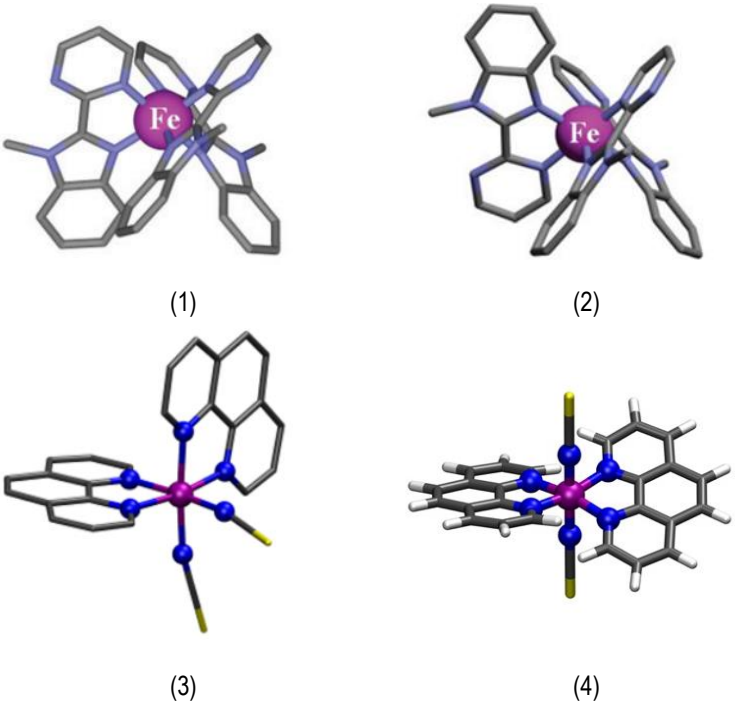

Figure 6. Representation of all the systems studied. (1): *fac*-$[Fe(L_1)_3]^{2+}$, (2): *mer*-$[Fe(L_1)_3]^{2+}$, (3): *cis*-$[Fe(phen)_2(NCS)_2]$, (4): *trans*-$[Fe(phen)_2(NCS)_2]$.

(1 and 2 extracted from Deorukhkar, N. et al. Dalton Transactions **2021**, 50(4), 1206–1223)
(*3 extracted from Cirera, J. et al. Inorganic Chemistry* ***2018****, 57(22), 14097–14105)*

Several parameters are calculated from these molecules. In the following table (Table 3) are collected the results obtained for the parameters calculated ΔE, ΔH, ΔS, $T_{1/2}$. The calculations have been carried out with the TPSSh functional and with a Def2TZVP basis. The experimental values for $T_{1/2}$ of molecules 1 and 2 are given with acetonitrile as the solvent, this fact has been considered at the time of calculation. Since the *trans*-$[Fe(phen)_2(NCS)_2]$ has not been extracted

from any article but has been drawn manually with the Gauss View program, there is no experimental value for its transition temperature.

System	ΔE [kcal/mol]	ΔH [kcal/mol]	ΔS [cal/K·mol]	$T_{1/2}$ [K] **calculated**	$T_{1/2}$ [K] [11-12] **experimental**
1 *in vacuum*	7.69	8.94	19.436	460	309
1 *in CH_3CN*	6.42	7.36	12.984	567	309
2 *in vacuum*	6.53	7.75	19.160	405	258
2 *in CH_3CN*	5.42	6.49	16.097	403	258
3	4.55	5.81	18.822	309	177
4	-1.65	-0.34	22.528	-15	-

Table 3. Summary of results for each molecule.

7.1. *FAC* VS. *MER* ISOMERS

Molecules 1 and 2 correspond to the *fac* and *mer* isomers respectively. The increase on the $T_{1/2}$ experimentally observed between *fac* and *mer* isomers is 51K, an increase that is properly reproduced by the calculations in vacuum (55K). However, the inclusion of solvent effects does not reproduce such trend (164K), in part due to the decrease in the ΔS for the *fac* isomer.

The increase in the $T_{1/2}$ can be explained by analyzing the electronic structures in terms of the relevant *d*-based molecular orbitals, for the *fac* isomer the ligand field splitting (Δ_{Oh}) has a value of 35096 cm^{-1}, while for the *mer* isomer it has a value of 34201 cm^{-1} for the same magnitude. This decrease of the Δ_{Oh} is responsible for providing a smaller $T_{1/2}$ value.

The molecular orbitals diagrams are enclosed in Appendix 2.

7.2. *CIS* VS. *TRANS* ISOMERS

Molecules 3 and 4 correspond to the *cis* and *trans* isomers respectively. In this case, molecule 3 is the only one extracted from the literature, molecule 4 was drawn manually as previously explained.

Focusing on the *trans* isomer it is confirmed that HS state is favored. The transition temperature is below 0K meaning the LS state would never exist on this system. Due to the geometry of the molecule (see Figure 4), axial thiocyanate groups create a strong anti-bonding interaction with two of the three t_{2g} orbitals and this causes an increase in their energy.

Consequently, the energy difference between the lowest unoccupied molecular orbital (LUMO) and the highest occupied molecular orbital (HOMO) greatly decreases, this reduction in the crystal field splitting is what favors the HS state (Figure 7).

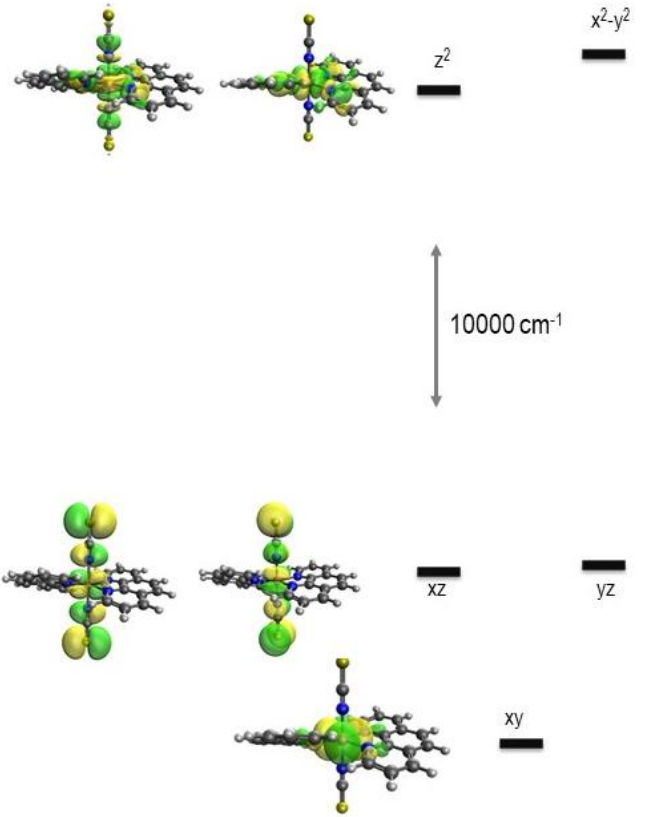

Figure 7. *trans*-[Fe(phen)$_2$(NCS)$_2$] MO diagram.

For the *cis* isomer, it can be noted that the $T_{1/2}$ calculated overestimates the experimental value. In this case, there is no axial interaction of the thiocyanates, which means that all orbitals are antibonding, but the splitting is much bigger (Figure 8).

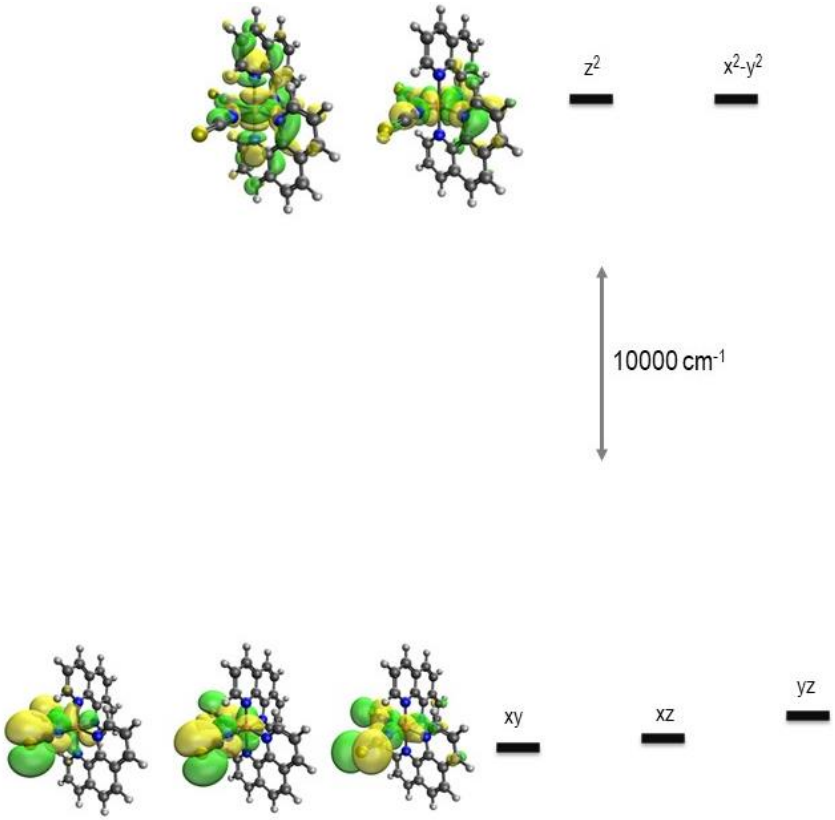

Figure 8. *cis*-[Fe(phen)$_2$(NCS)$_2$] MO diagram.

9. CONCLUSIONS

During the project, four Iron (II) complexes have been studied using Density Functional Theory methods.

First, a methodological exploration to select the optimal functional and basis set was done on the *fac*-$[Fe(L_1)_3]^{2+}$ and *mer*-$[Fe(L_2)_3]^{2+}$ system. Our results indicate that TPSSh/Def2TZVP is a suitable method to reproduce the experimental $T_{1/2}$ in such system, although other functionals (B3LYP* and OPBE) could potentially be used for the same purpose.

The TPSSh/Def2TZVP method was later used to reproduce the experimentally observed differences in the systems *fac*-$[Fe(L_1)_3]^{2+}$ and *mer*-$[Fe(L_1)_3]^{2+}$. The results in vacuum nicely reproduce the experimental trend, which can be understood by analyzing the electronic structure of the system. Similarly, we also studied the effect of the cis/trans configuration in the $[Fe(phen)_2(NCS)_2]$ system, which shows stabilization of the high-spin state in the *trans*-isomer due to strong antibonding character gained by the *d*xz/*d*yz pair of orbitals.

From the above, it is possible to state that electronic structure calculations at the TPSSh/Def2TZVP level can reproduce and explain experimental trends in SCO systems that differ in their stereochemistry, which validates the method for in silico screening of new members of such families, including the possibility of ruling out systems that lost the SCO behavior.

10. REFERENCES AND NOTES

1. Take action for the sustainable development goals - United Nations Sustainable Development. United Nations Sustainable Development. https://www.un.org/sustainabledevelopment/sustainable-development-goals/ (accessed December 29, 2023).
2. Gütlich, P., Spin Crossover – Quo Vadis? *Eur. J. Inorg. Chem.* **2013**: 581-591.
3. Nicolazzi, W., & Bousseksou, A., Thermodynamical aspects of the spin crossover phenomenon. *Comptes Rendus Chimie* **2018**, 21(12), 1060–1074.
4. Shao D, Shi L, Yin L, Wang BL, Wang ZX, Zhang YQ, Wang XY., Reversible on-off switching of both spin crossover and single-molecule magnet behaviours via a crystal-to-crystal transformation. *Chem Sci.* **2018**, 9(41), 7986-7991.
5. Dalal, M.; A Textbook of Inorganic Chemistry, *Dalal Institute;* 1st ed.; 2017; 354-358.
6. Tesfaye, D., Linert, W., Gebrezgiabher, M., Bayeh, Y., Elemo, F., Sani, T., Kalarikkal, N., & Thomas, M., Iron (II) Mediated Supramolecular Architectures with Schiff Bases and Their Spin-Crossover Properties. *Molecules* **2023,** Vol. 28, Issue 3.
7. Muller, R.N., Elst, L. V., Laurent, S., Spin transition molecular materials: intelligent contrast agents for magnetic resonance imaging. *J. Am. Chem. Soc.* **2003,** 125, 8405.
8. Kumar, K. S., & Ruben, M., Sublimable Spin-Crossover Complexes: From Spin-State Switching to Molecular Devices. *Angewandte Chemie International Edition* **2017**, 60(14), 7502–7521.
9. Orio, M., Pantazis, D. A., & Neese, F., Density functional theory. *Photosynthesis research*, **2009**, 102(2–3), 443–453.
10. Harrison, N. M., An Introduction to Density Functional Theory. *Advances in Materials Physics and Chemistry*, **2017**, Vol.11 No. 1.
11. Deorukhkar, N., Besnard, C., Guénée, L., & Piguet, C., Tuning spin-crossover transition temperatures in non-symmetrical homoleptic meridional/facial $[Fe(didentate)_3]^{2+}$complexes: what for and who cares about it? *Dalton Transactions* **2021**, 50(4), 1206–1223.
12. Cirera, J., Via-Nadal, M., & Ruiz, E., Benchmarking Density Functional Methods for Calculation of State Energies of First Row Spin-Crossover Molecules. *Inorganic Chemistry* **2018**, 57(22), 14097–14105.

11. ACRONYMS

SCO: Spin Crossover

HS: High-Spin

LS: Low-Spin

ST: Spin Transition

DFT: Density Functional Theory

LDA: Local Density Approximation

GGA: Generalized Gradient Approximation

HF: Hartree-Fock

TPSSh: Tao-Perdew-Staroverov-Scuseria hybrid

MO: Molecular Orbitals

Phen: phenanthroline

L_1: 1-methyl-2-(pyrimidin-2-yl)-1*H*-benzo[*d*]imidazole

L_2: 1-methyl-2-(pyrimidin-4-yl)-1*H*-benzo[*d*]imidazole

APPENDICES

APPENDIX 1: PYTHON PROGRAM

```python
#Programa python version 1 per llegir dades de sortida de output freq gaussian

#Importem moduls
import numpy as np
import math
import matplotlib.pyplot as plt

#Definition of constants
kb=1.380649E-23 # J·K
hplanck=6.62607015E-34 # J·s-1
T=10 # K
au2kcalmol=627.509541 # Conversion to kcal/mol
J2kcalmol=1.44E20 # conversion to kcal/mol
R=1.98720425864083E-3 #gas constant in kcal/mol·K
mHS=math.sqrt(4.0*(4.0+2.0))

#Reading freqs from high-spin
freq_hs=np.loadtxt("freq_ikixuy_hs_ch3cn.txt")

#Reading freqs from low-spin
freq_ls=np.loadtxt("freq_ikixuy_ls_ch3cn.txt")

#Reading energies from high-spin
Energy_hs=np.loadtxt("thermochem_ikixuy_hs_ch3cn.txt")
energy_hs_zpe=Energy_hs[0]
energy_hs_T=Energy_hs[1]
energy_hs_H=Energy_hs[2]
energy_hs_G=Energy_hs[3]

#Reading energies from low-spin
Energy_ls=np.loadtxt("thermochem_ikixuy_ls_ch3cn.txt")
energy_ls_zpe=Energy_ls[0]
energy_ls_T=Energy_ls[1]
energy_ls_H=Energy_ls[2]
energy_ls_G=Energy_ls[3]

print("Electronic Energy Low-spin", energy_ls_zpe)
print("Lowest low-spin freq:", freq_ls[0])
print("Electronic Energy High-spin", energy_hs_zpe)
print("Lowest high-spin freq:", freq_hs[0])

#Requesting user data
T0=float(input("Insert initial T[K]: "))
#print(T0)
Tf=float(input("Instert final T[K]: "))
#print(Tf)
n_p=int(input("Insert number of points on the interval: "))
#print(n_p)
interval_T=np.linspace(T0,Tf,n_p)
#print(interval_T)

#Definition of G vectors
G_ls=np.zeros(len(interval_T))
G_hs=np.zeros(len(interval_T))
```

```
55
56 #Looping over the Tempereature
57 for j in range(len(interval_T)):
58
59     #Attempt to compute G_ls for all freq
60     in_sum=0.0E0
61     for i in range(len(freq_ls)):
62         in_sum=in_sum+math.log(1-math.exp(-((hplanck*freq_ls[i])/(kb*interval_T[j]))))
63
64     #print("sum[ln(1-e^(h·vi/kB·T))]=",in_sum)
65     G_T_lowspin=Energy_ls[0]*au2kcalmol+kb*interval_T[j]*J2kcalmol*in_sum
66 #    print("G_ls",interval_T[j],"= ",G_T_lowspin)
67     G_ls[j]=G_T_lowspin
68
69 #print(G_ls)
70
71 #Looping over the Temperature
72 for j in range(len(interval_T)):
73
74     #Attempt to compute G_hs for all freq
75     in_sum=0.0E0
76
77     for i in range(len(freq_hs)):
78         in_sum=in_sum+math.log(1-math.exp(-((hplanck*freq_hs[i])/(kb*interval_T[j]))))
79
80     #print("sum[ln(1-e^(h·vi/kB·T))]=",in_sum)
81     G_T_highspin=Energy_hs[0]*au2kcalmol+kb*interval_T[j]*J2kcalmol*in_sum
82 #    print("G_hs",interval_T[j],"= ",G_T_highspin)
83     G_hs[j]=G_T_highspin
84 #Computing DG at a given T
85     G_T=G_hs-G_ls
86     G_T[j]=G_hs[j]-G_ls[j]
87 #    print("DG(T)",G_T)
88
89 #Trying to find transition Temperature
90 j=0
91 while G_T[j]>0:
92     j = j +1
93     index=j
94
95 #print(G_T[index],G_T[index-1])
96 print("T1/2 =",((interval_T[index]+interval_T[index-1])/2.0))
97
98 #Computing DG at a given T
99 #    G_T=G_hs-G_ls
100  #   G_T[j]=G_hs[j]-G_ls[j]
101 #    print("DG(T)",G_T)
102
103 #Converting DG to Keq
104 Keq=np.exp(-G_T/(R*interval_T))
105 #print(Keq)
106 #Converting Keq to gamma_hs
107 gamma_hs=Keq/(1.0+Keq)
108 #print(gamma_hs)
109 #Converting gamma to magnetic moment
110 meff_HS = gamma_hs*mHS
111
112 #Trying to draw
113 plt.plot(interval_T,meff_HS)
114 plt.ylabel("μeff")
115 plt.xlabel("T/K")
116 plt.title("Representation μeff vs. T", fontsize=10, horizontalalignment="right")
117 plt.savefig("PLOT_ikixuy_ch3cn.jpeg")
118 plt.show()
119
```

APPENDIX 2: MO DIAGRAMS: *FAC* AND *MER* ISOMERS

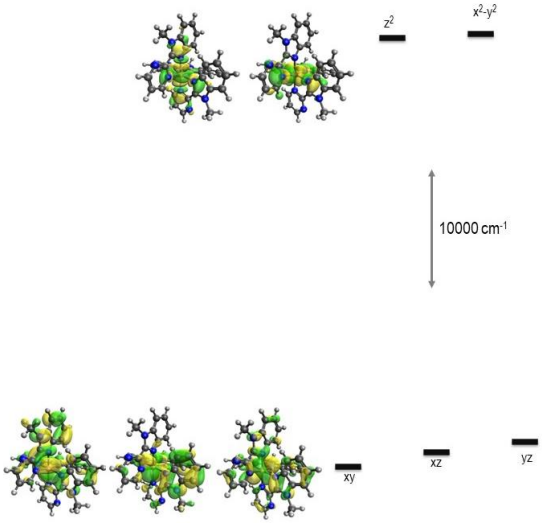

Figure 9. MO diagram of *fac*-$[Fe(L_1)_3]^{2+}$ in vacuum.

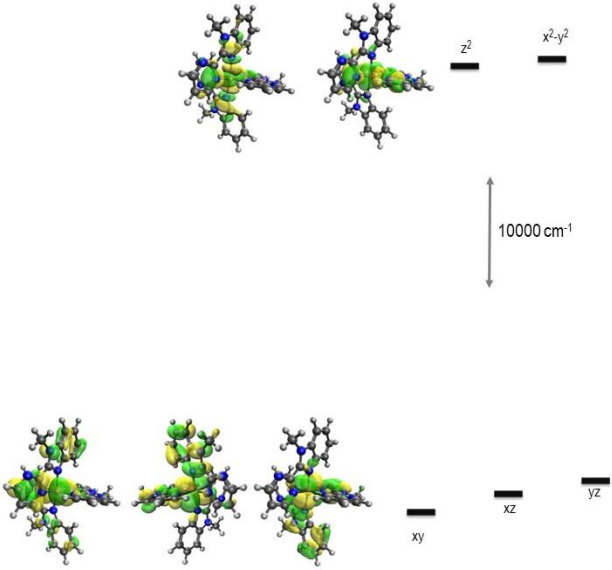

Figure 10. MO diagram of *mer*-$[Fe(L_1)_3]^{2+}$ in vacuum.

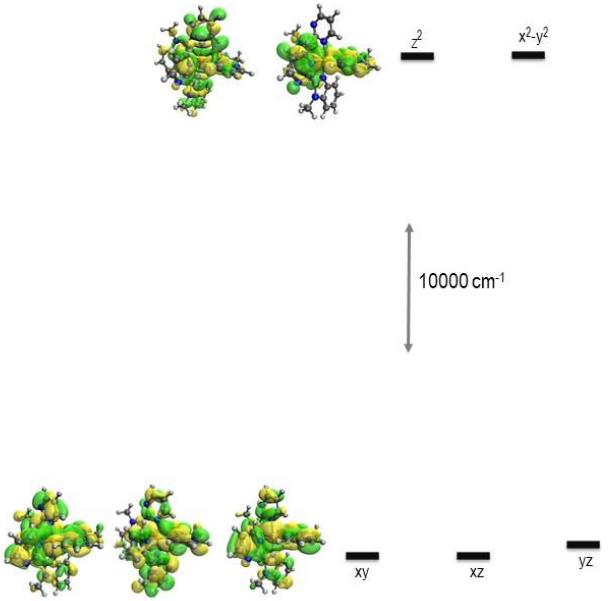

Figure 11. MO diagram of *fac*-$[Fe(L_1)_3]^{2+}$ in CH_3CN.

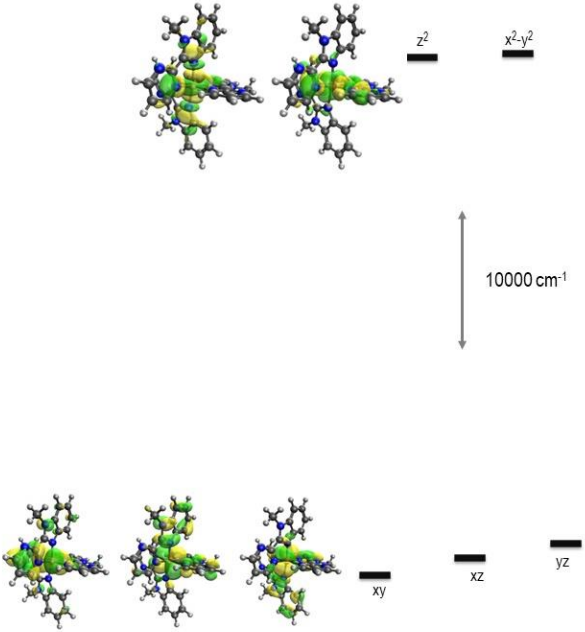

Figure 12. MO diagram of *mer*-$[Fe(L_1)_3]^{2+}$ in CH_3CN.